Organisms Diversity & Evolution (2024) 24:67–83
https://doi.org/10.1007/s13127-023-00633-8

ORIGINAL ARTICLE

Hardly Venus's servant—morphological adaptations of *Veneriserva* to an endoparasitic lifestyle and its phylogenetic position within Dorvilleidae (Annelida)

Ekin Tilic[1,2] · **Greg W. Rouse**[3]

Received: 18 September 2023 / Accepted: 30 November 2023 / Published online: 16 January 2024

Abstract
Endoparasitic annelids living inside another annelid host are known, particularly with regard to Oenonidae, but in general are poorly studied. The dorvilleid *Veneriserva pygoclava* is known from southern California, and its genus name (Latin = Venus's servant) alludes to the close association with the host aphroditid scaleworm *Aphrodita longipalpa*. Little is known on fundamental questions on the biology of *Veneriserva pygoclava*. What is its mode of reproduction? How do they feed? How do they penetrate the host? We have studied multiple parasitized hosts and *V. pygoclava* specimens, using an integrative approach, combining µCT, histology, and electron microscopy. 3D reconstructions from µCT data of a parasitized *Aphrodita* show the exact position of the parasites in their natural condition within the host's coelomic cavity. Ultrastructural investigations of the parasites revealed interesting adaptations to their lifestyle such as the complete reduction of their gut, despite the presence of a functional jaw apparatus and a modified epidermis enabling nutrient uptake from the host's coelomic fluid. In addition to these, we also investigated spermatogenesis and oogenesis in *V. pygoclava*. Sperm morphology indicates an external fertilization of eggs within the coelomic cavity of the host. Mature male and female parasites living inside the same mature host and the presence of juvenile *V. pygoclava* within juveniles of *Aphrodita* suggest an obligate form of parasitism with a very early penetration of the hosts. In addition to our detailed morphological investigation, we conducted a phylogenetic analysis showing the position of *Veneriserva* within Dorvilleidae and its position was recovered nested among taxa of the *Iphitime*. Our phylogenetic analyses also show that the taxation *Ophryotrocha puerilis siberti* should be given full species rank and referred to as *Ophryotrocha siberti*. Finally, we publish here the full mitochondrial genome of *V. pygoclava* and discuss its novel gene order with reference to other annelids.

Keywords Ultrastructure · Micro-CT · Parasite · *Aphrodita* · Mitochondrial genome · Phylogeny

Introduction

Rossi (1984) described *Veneriserva pygoclava* Rossi, 1984 from southern California, giving it the allusive genus name (Latin = Venus's servant), referring to their close association with *Aphrodita longipalpa* Essenberg, 1917, a sea mouse (Aphroditidae). Apart from the original species description by Rossi (1984) and the ecological studies on the Antarctic subspecies *V. pygoclava meridionalis* by Micaletto et al. (2002) and Micaletto et al. (2003), no other study exists on these endoparasitic annelids that live within the coelomic cavity of their hosts. *Veneriserva* is the only known member of Dorvilleidae that is endoparasitic. However, numerous Dorvilleidae species, primarily from the genus *Iphitime*, as well as some from *Ophryotrocha*, exhibit ectoparasitic or commensal relationships with decapod crustaceans (Martin & Britayev, 1998).

Polychaetes that parasitize other polychaetes had been, until recently, only restricted to some members of Oenonidae and *Veneriserva* (Jimi et al., 2021; Martin & Britayev, 1998, 2018). *Endovermis seisuiae* Jimi et al. 2020, an endoparasitic Phyllodocidae from Japanese waters, with *Aphrodita* and

✉ Ekin Tilic
ekin.tilic@senckenberg.de

✉ Greg W. Rouse
grouse@ucsd.edu

[1] Department of Marine Zoology, Senckenberg Research Institute and Natural History Museum, Frankfurt, Germany

[2] Institute of Evolutionary Biology and Animal Ecology, Rheinische Friedrich Wilhelms Universität, Bonn, Germany

[3] Scripps Institution of Oceanography, University of California San Diego, La Jolla, CA, USA

Lepidonotus spp. hosts, is the most recent addition to this very short list (Jimi et al., 2021). Much of the research up to now has been restricted to taxonomic descriptions and far too little attention has been paid to fundamental questions on the biology of endoparasitic polychaetes. This is also largely because parasitic Oenonidae often have a free-living stage and lack any pronounced morphological adaptations (Emerson, 1974; Hernández-Alcántara & Solís-Weiss, 1998; Pettibone, 1957). Also, in the case of the recently described *Endovermis*, nothing is known on the mechanisms of host entry, reproduction, and feeding (Jimi et al., 2021).

Endoparasitic organisms occupy one of the most specialized ecological niches, residing within the body of another organism. This intimate relationship with the host usually demands a suite of adaptations, often driving significant morphological changes. To thrive in such a unique environment, endoparasites must navigate and withstand the host's defense mechanisms. A resilient tegument, such as the neodermis in adult parasitic flatworms (Tyler & Tyler, 1997), or parasite encystment, like in the notorious nematode *Trichinella spiralis* (Ritterson, 1966), can aid in resisting digestive enzymes and immune attacks (Zarowiecki & Berriman, 2015). Adaptations for nutrient uptake within a host, like the tegument brush border of tapeworms that amplifies the surface area by 10 to 50 times (Lumsden, 1975), are also crucial. These examples, all driven by the need to survive and reproduce in the challenging internal environment of a host, suggest that *Veneriserva* likely evolved set of morphological traits enabling them to thrive within the coelomic cavity of their polychaete hosts.

This paper seeks to unravel some of these mysteries surrounding the biology of *Veneriserva* using a holistic approach integrating a variety of morphological (µCT, TEM, and histology) and molecular techniques. We not only demonstrate unique anatomical adaptations to a parasitic lifestyle but also publish the full-mitochondrial genome of these fascinating and understudied annelids. Furthermore, we discuss the phylogenetic placement of *Veneriserva* within Dorvilleidae, based on a five-gene molecular phylogeny.

Material and methods

Specimens

Specimens of *Aphrodita longipalpa* were obtained from near its type locality off San Diego by otter trawl at depths of 500–700 m depth on soft bottom from 2017 to 2022. The specimens were identified as *A. longipalpa* based on its distinctly elongate palps. Vouchers have been deposited at the Benthic Invertebrate Collection of Scripps Institution of Oceanography (SIO-BIC) and at the Senckenberg Natural History Museum, Frankfurt (SMF).

Aphrodita longipalpa specimen vouchers: SIO-BIC A7408, A10919 (µCT), A13898, A14143, A14144 (CO1 barcode sequence on GenBank: OR544434) and histologically sectioned juveniles with *Veneriserva* SMF 32800, SMF32801, and SMF 32802.

Veneriserva pygoclava specimen vouchers: SIO-BIC A7406, A7409, A11479, A13465, A13466, A16364, A16365, A16366, A16372 (CO1 barcode: OR826119), A16373 (CO1 barcode: OR826119), A16374 (CO1 barcode: OR826117), A18367, and A13687 (mitogenome on GenBank: OR449961, CO1 barcode: OR826118).

Micro-computed tomography (µCT)

An adult sized specimen of formalin-fixed, ethanol-preserved *A. longipalpa* was chosen for µCT scanning (SIO-BIC A10919). The specimen was stained with a contrast enriching phosphotungstic acid solution (0.3% PTA in 70% ethanol) (Metscher, 2009) for 3 weeks before scanning. A SkyScan 1272 µCT scanner (Bruker microCT, Kontich, Belgium) was used with the following parameters: 60 kV source voltage, 166 µA source current, 972 ms exposure, and a camera resolution of 1224 × 820 px. The voxel resolution was 7.4 µm. An aligned image stack was generated with the software Nrecon (Bruker) and the surface renderings were generated with the software Drishti 2.6.5 (Limaye, 2012) (National University, Canberra, Australia). 3D reconstructions were done using Amira 6.7 (FEI Company, Hillsboro, OR, USA).

The entire µCT dataset is published together with this paper and is available under https://doi.org/10.5281/zenodo.8260723.

Semi-thin histology and transmission electron microscopy (TEM)

Male and female *Veneriserva pygoclava* used for TEM and semi-thin histology were directly dissected into the fixative and fixed in 2.5% glutaraldehyde buffered in 0.05 M phosphate 0.3 M NaCl saline (PBS) for 1–2 h in room temperature. The samples were rinsed and stored in PBS (with NaN_4) until embedding. The samples were postfixed with 1% OsO_4, buffered in the same way as the fixative, for 30 min at 4 °C. The material was subsequently dehydrated in an ascending alcohol series and embedded in Spurr's low viscosity embedding mixture. Series of silver interference-colored ultra-thin sections (60–70 nm) were prepared with a Diatome Ultra 45° diamond knife mounted on a Leica Ultracut S ultramicrotome and placed on formvar-covered single-slot copper grids. These were stained with 2% uranyl acetate and 2.6% lead citrate (E17810, Science Services) after Reynolds in an automated TEM stainer (QG-3100,

Boeckeler Instruments). Ultra-thin sections were examined and imaged using a ZEISS EM10CR with phosphate imaging plates (Ditabis). Ribbons of 1-µm semi-thin sections were prepared with a Diatome Histo 45° diamond knife on the same microtome and collected on object slides following Blumer et al. (2002). Semi-thin sections were stained with toluidine blue (1% toluidine, 1% sodium tetraborate, and 20% sucrose) and the coverslips were mounted with Araldite. These were imaged using an Olympus BX-51 microscope with an Olympus CC12 camera setup.

Paraffin histology

Two formalin-fixed juveniles of *A. longipalpa* were post-fixed for 24 h in Bouin's solution (modified after Dubosque-Basil). The specimens were dehydrated completely in an ascending ethanol series, followed by an incubation in methylbenzoate and subsequently in butanol. The material was preincubated in Histoplast (Thermo Scientific, Dreieich, Germany) at 60 °C for 2 weeks and multiple medium changes and later embedded in Paraplast (McCormick Scientific, Richmond, USA). Serial sections of 7 µm thickness were prepared using an Autocut 2050 microtome (Reichert-Jung, Leica, Wetzlar) and transferred on to glass slides coated with albumen-glycerin. Sections were stained with Azan staining (stained with carmalaun, subsequently differentiated with a 5% phosphotungstic acid solution, washed in distilled water, and stained again with an aniline blue-orange G mixture). Coverslips were mounted using malinol.

Complete series of the two parasitized *A. longipalpa* specimens are deposited in the Senckenberg Natural History Museum, Frankfurt am Main, Germany (collection numbers SMF 32800, SMF32801, and SMF 32802).

Phylogenetic analysis

DNA sequences of the mitochondrial gene 16S rRNA (16S), cytochrome c oxidase subunit I (COI), cytochrome b (Cytb), and the nuclear genes 18 rRNA (18S) and histone H3 (H3) for a wide range of Dorvilleidae were sourced from GenBank (Supplementary Table 1) and used with newly generated sequences for *Veneriserva pygoclava*. The new sequences were obtained following the same protocols and primers outlined in Yen and Rouse (2020). A eunicid, *Eunice pennata* (Müller, 1776), was used as the outgroup. Alignments were performed using MAFFT (Katoh & Standley, 2013). A maximum likelihood (ML) analysis was conducted using RAxML-NG (Kozlov et al., 2019) and ModelTest-NG (Darriba et al., 2020) in the raxmlGUI 2.0 interface (Edler et al., 2021). The models used for each partition were chosen in ModelTest-NG and the partitions were concatenated. Fifty random addition searches were run to obtain the maximum likelihood tree and 1000 bootstrap pseudoreplicates were generated and analyzed to assess support. The resulting best tree with bootstrap scores was visualized with FigTree 1.4.4 (Rambaut, 2018). A haplotype network of five *Veneriserva pygoclava* COI sequences was created with PopART ver. 1.7 (Leigh & Bryant, 2015) using the TCS algorithm.

Mitochondrial genome assembly

DNA was extracted from several specimens of *Veneriserva pygoclava* using the Zymo Research DNA-Tissue Miniprep kit. DNA quantity was estimated using a Qubit dsDNA BR Assay Kit with a Qubit fluorometer (Invitrogen). The DNA extraction with the highest concentration (SIO-BIC A13687) was chosen for genome skimming. Library preparation and sequencing was carried out by Novogene Corporation Inc. (Sacramento, CA). Whole genome libraries were prepared targeting an insert size of 350 bp. A total of 9,303,989 paired-end reads (150 bp) were sequenced on an Illumina NovaSeq 6000. Raw sequence reads were uploaded to the NCBI SRA database and are available under the BioProject accession number: PRJNA1041643.

The complete circular mitochondrial genome was assembled with GetOrganelle v1.7.5.2 (Jin et al., 2020), which uses a "baiting and iterative mapping" approach to de novo assemble circular organelle genomes. The GetOrganelle pipeline incorporates Bowtie2 (Langmead & Salzberg, 2012) and SPAdes (Bankevich et al., 2012). The average base coverage for the mitogenome assembly was 974 and the average kmer coverage was 155.8. The assembled mitochondrial genome was first annotated on the MITOS2 web server (RefSeq 81 Metazoa; Genetic Code 9) (Donath et al., 2019) and then manually with Geneious Prime® 2022.0.1. NCBI GenBank accession number for the complete mitochondrial genome of *Veneriserva pygoclava* is OR449961. The mitochondrial genome map was drawn using Organellar Genome Draw (ORGDRAW) (Lohse et al., 2007).

Results

Parasite abundance

Often the parasites could be observed moving within the host's body when the more translucent ventral side of the sea mice were inspected (Fig. 1A) or dorsally when the felt-age chaetae were removed (Fig. 1B). Male *V. pygoclava* are markedly smaller in size when compared to their female counterparts (Fig. 1F, G) and are easy to overlook. Males were almost entirely white whereas the females had an anterior white mark and an orange mid-dorsal line (Fig. 1D–G).

The infection rate of *A. longipalpa* with *V. pygoclava* appears to be high, at least in the specimens collected off San Diego. A total of 61 specimens of *A. longipalpa* were

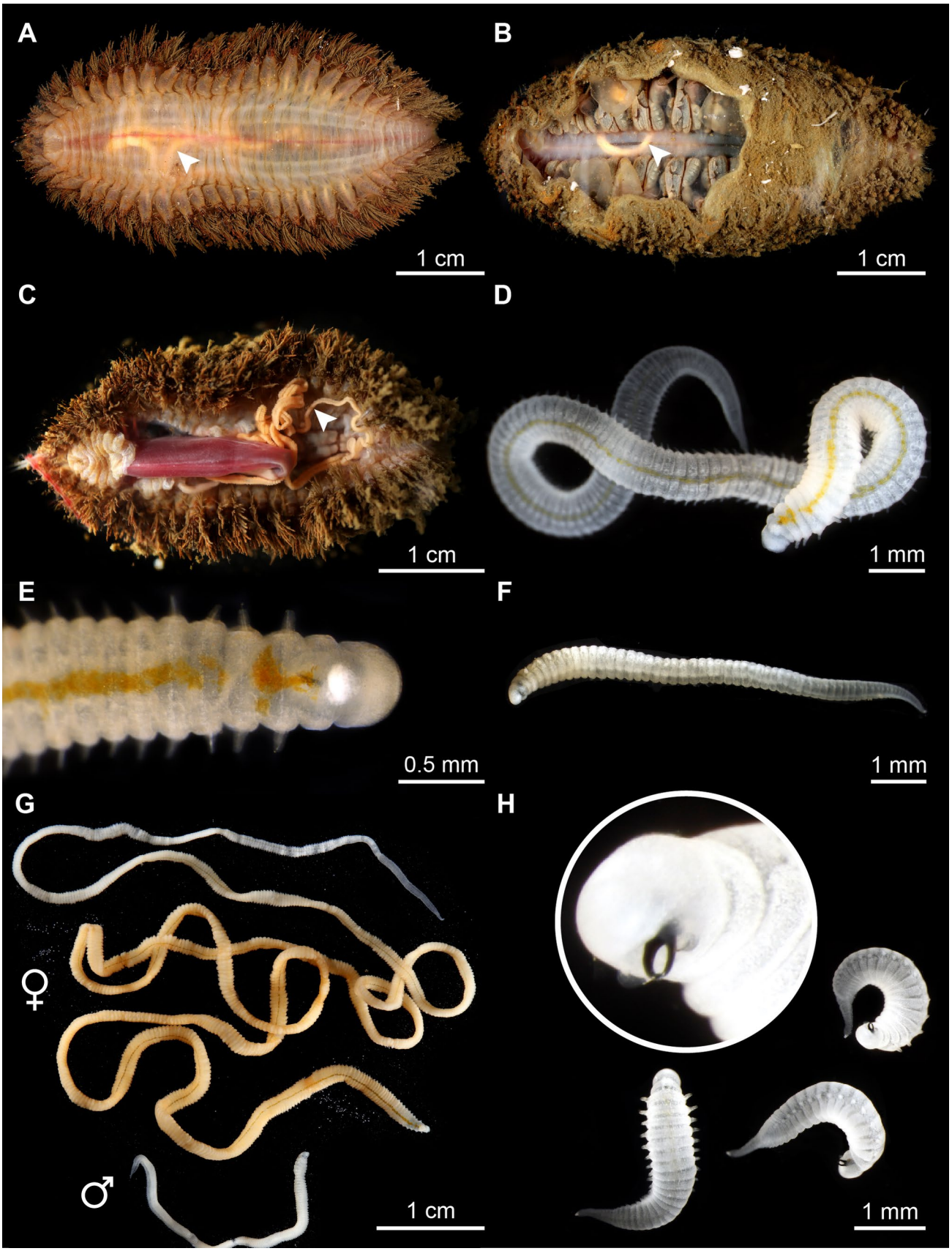
A
1 cm
B
1 cm
C
1 cm
D
1 mm
E
0.5 mm
F
1 mm
G
♀
♂
1 cm
H
1 mm

◂**Fig. 1** Live photos and dissection of parasitized *Aphrodita longipalpa* and *Veneriserva pygoclava*. **A** Ventral view of *A. longipalpa*. **B** Dorsal view of *A. longipalpa* with removed feltage chaetae, revealing the parasite visible through the body wall. **C** Ventrally dissected *A. longipalpa*, exposing the sizable female parasite. *Veneriserva pygoclava* individuals within the host are indicated by arrowheads. **D** Juvenile female *V. pygoclava*, with developing oocytes visible through the body wall along the mid-dorsal orange line. **E** Female *V. pygoclava* showing the mid-dorsal orange pigmentation and the white mark at the base of the prostomium. **F** Male *V. pygoclava*. **G** A large female and smaller male *V. pygoclava*, extracted from the same host. The pygidium is club-shaped in both males and females and juveniles. **H** Juvenile *V. pygoclava* shown from multiple angles, characterized by a complete white coloration; black jaws are magnified in panel

collected by trawling during several cruises in the years between 2017 and 2022. Out of the 58 dissected specimens, 62% were found to be parasitized (Fig. 2). Among the remaining three specimens, one was scanned using microCT, and two were histologically sectioned, revealing the presence of parasites in all three cases, which makes a total 64% of specimens of *A. longipalpa* parasitized by *V. pygoclava*. Of the dissected individuals, 24% exhibited a male and a female *V. pygoclava* cohabiting within a single host. Solitary female parasites were found in 17% of the specimens; six individuals of *A. longipalpa* (10%) housed a single female coexisting with two males. Additionally, one *A. longipalpa* featured a female cohabiting with a single juvenile. The remaining 9% of cases consisted of solitary juveniles (Fig. 2). The presence of parasites showed a significant correlation with host size, indicating that larger hosts were more prone to parasitization (*t*-test *p* value: 2e − 04). Additionally, hosts hosting both female and male parasites exhibited larger sizes. Specimens of *Aphrodita* that accommodated 3 parasites (one female + two males) surpassed the size of those with only a male and female *V. pygoclava*. Interestingly, sea mice hosting juvenile parasites were comparatively smaller (see Fig. 2). Similar infection rates were observed in specimens collected in October and May.

Position of *Veneriserva* within *Aphrodita*

The µCT scan of a parasitized *A. longipalpa* allowed visualizing in 3D the position of *Veneriserva* inside their host without dissection and in their natural condition (Fig. 3). In the *Aphrodita* specimen scanned, a single juvenile and a single female *V. pygoclava* were present. The juvenile is likely to be a male, as two females were never observed together in a single host. *Veneriserva pygoclava* resided within the coelomic cavity of the host, largely occupying the lateral and ventral coelomic spaces (Fig. 3). The larger female was approximately 77.1 mm long, 10 times the size of the juvenile (± 7.2 mm), and about twice the length of the host (± 42.7 mm) (Fig. 3A). The female was positioned in a U-shaped coil with the posterior and anterior ends both located near the anterior of the host. The juvenile was located near the anterior end of the female (Fig. 3A, B, E, F). Other female *Veneriserva* with an even larger parasite to host body length ratio were observed in some of the dissected specimens (Fig. 1C, G). In these, the parasites could be observed making multiple coils within the ventral coelomic space, and also extending dorsally (Fig. 1A–C), taking up a very large area within the host's body. Neither the musculature nor the gut of the host appeared to be substantially damaged by the parasite (Fig. 3B–D). Despite the relatively large size of many of the *A. longipalpa* collected, no gonads or gametes of any stage were observed in any sampled hosts, infected or not. Specimens were observed from the months December, March, May, July, September, and October over the period of 2017 to 2023; so, the breeding season may be over the winter/spring months.

Interestingly, the two juvenile *A. longipalpa* specimens examined (both less than 3 cm in length) did not show any signs of infection upon external inspection of the ventral side. However, histological sectioning of these specimens revealed a single juvenile *V. pygoclava* in both (Fig. 4A, B). These *V. pygoclava* specimens were juveniles themselves and did not show any signs of gametogenesis (Fig. 4B), so sex determination was not possible.

Oogenesis

Oogenesis in *Veneriserva pygoclava* occurs in segmentally repeated ovaries. The oogonia of *V. pygoclava* proliferated from the ventral surface of the dorsal blood vessel (Fig. 5A, C) and the gonads were attached to the intersegmental septa (mesenteries) (Fig. 5C). Each developing oocyte was directly connected to a nurse cell by intercellular cytoplasmic bridges (Fig. 5D). The nucleus of the oocyte appeared to undergo numerous morphological changes during oogenesis, as it appeared heterochromatic in early stages and enlarged and became euchromatic with a single prominent nucleolus during the vitellogenic phase (Fig. 5B, C). The nurse cells appeared to undergo a striking morphological change after the onset of vitellogenesis, making them easy to distinguish from their neighboring oocytes. During vitellogenesis, the volume of the nurse cell nucleus rapidly increased and was always dense and heterochromatic, whereas the nuclei of the oocytes were all euchromatic at this stage (Fig. 5C). Another difference between vitellogenic oocytes and nurse cells was the size and distribution of yolk platelets. Nurse cells never contained ripe yolk bodies, but only small-sized yolk platelets arranged in clusters (Fig. 5D). While oocytes kept growing reaching a final diameter of about 100 µm, nurse cells had already reached their final diameter of about 30 µm during vitellogenesis. The nurse cells then appear to undergo a decrease in diameter until they are finally incorporated into the oocytes (Fig. 5B).

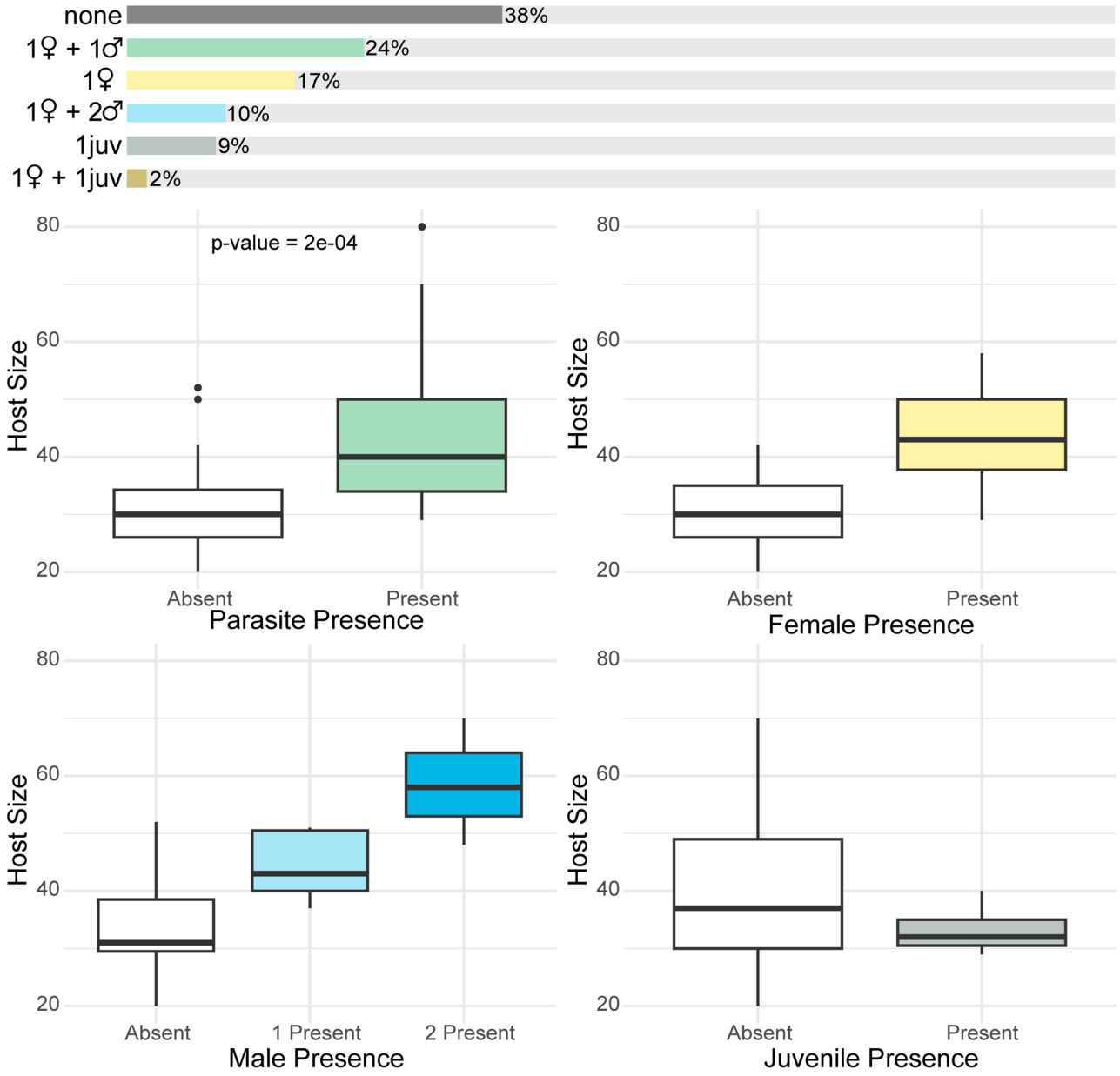

Fig. 2 Parasite abundance and distribution statistics. A total of 58 *Aphrodita longipalpa* were dissected and examined for parasite presence. The upper horizontal bars graphically depict the proportional parasitism rates and the corresponding distribution among male, female, and juvenile parasites, along with various cohabitation configurations. The box plots show the relationship between host size and the occurrence of parasites, presented collectively and then individually for female, male, and juvenile parasites

Spermiogenesis

In the histologically sectioned male specimen, spermiogenesis occurred along the peritoneal lining (Fig. 5F). Spermatogonia were found ventrally associated with the coelomic lining, near the dorsal blood vessel (Fig. 5F). Spermatocytes and mature sperm were found released into the coelomic cavity. Upon dissection, liberated sperm cells could be observed under the light microscope. Mature sperm of *V. pygoclava* had a large conical acrosome (~ 12 µm long) and a spherical nucleus (6 µm in diameter) with no evidence of an emergent flagellum (Fig. 5E).

Pharyngeal apparatus and lack of an intestine

The alimentary tract of *V. pygoclava* was found to be unique and aberrant among Annelida, in that it consisted of a functional muscular axial proboscis with a jaw apparatus but with no through-gut (Figs. 3E, and 4B–H). The pharynx ended blindly (Fig. 4G, H) leaving a completely

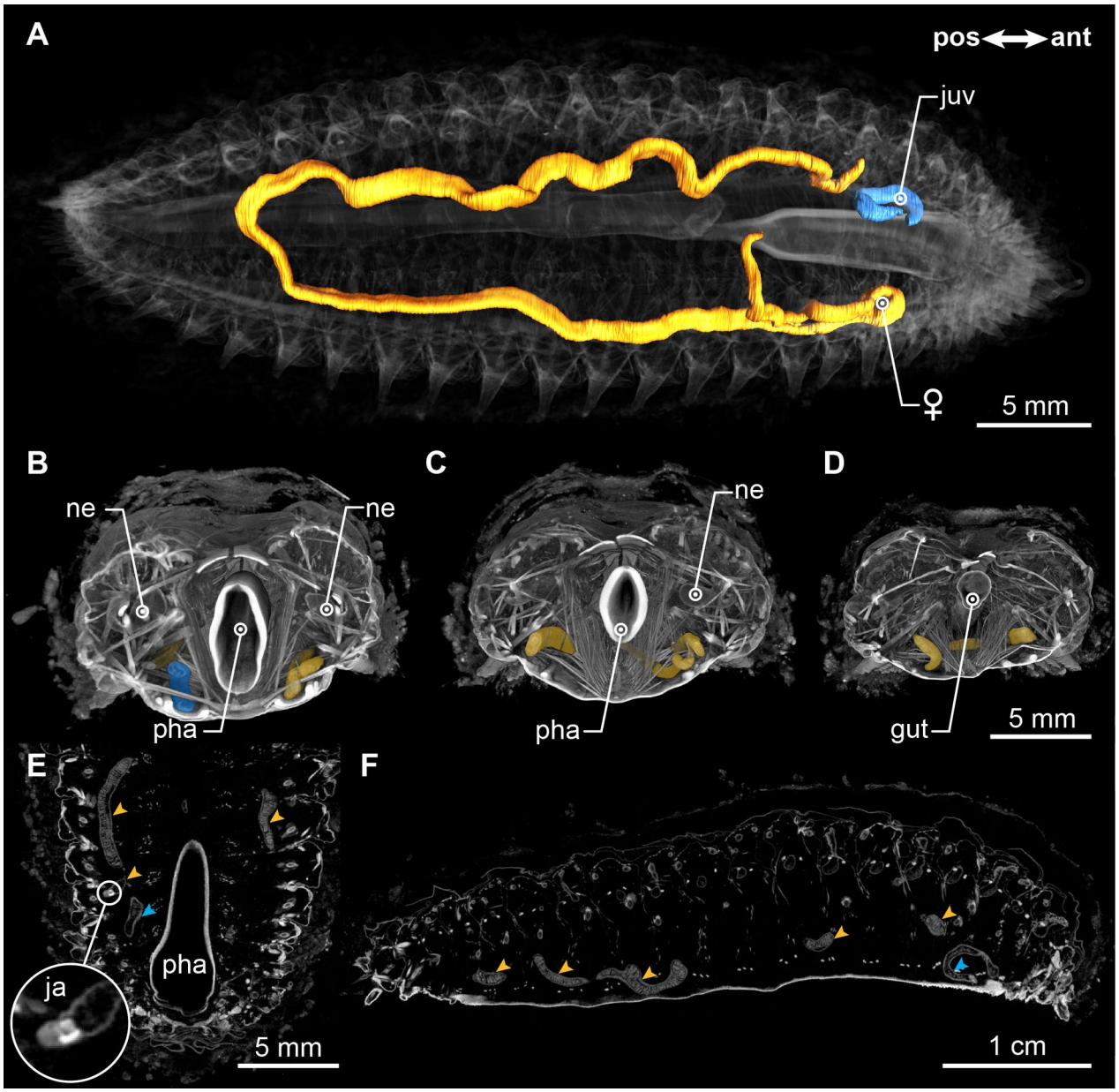

Fig. 3 µCT visualization of parasites within *Aphrodita longipalpa*. **A** 3D rendering of parasites shown within the projection of the host body. **B–D** Virtual dissections of surface renderings, showing cross-sections of the host across three consecutive body regions, from anterior to posterior. Raw image data from the micro-CT stack, illustrating a horizontal section through the host (**E**) and a sagittal section (**F**). Head of the juvenile parasite is magnified to display the prominent jaws in white. Abbreviations—*ja* jaws, *ne* nephridia, *pha* pharynx. Female *Veneriserva pygoclava* is shown in yellow or with yellow arrowheads and the juvenile *V. pygoclava* in blue or with blue arrowheads

hollow body cavity only occupied by developing gametes in mature specimens (Fig. 5A, F). The complete reduction of the gut was observed in both juvenile (Fig. 4B–H) and adult specimens of *V. pygoclava* (Fig. 5A, F) we sectioned histologically. Even though a jaw apparatus is present, and the animals can evert and move the maxillae in a pinching motion (Fig. 1H). The maxillae and the fused mandibles appear reduced when compared to free-living Dorvilleidae. The pygidium of *V. pygoclava* was confirmed as being club shaped, which inspired the species epithet. An anus, rudimentary or not, was not confirmed.

Epidermal ultrastructure

The entire body surface of *V. pygoclava* was densely covered with microvilli of the epidermal cells that pierced through

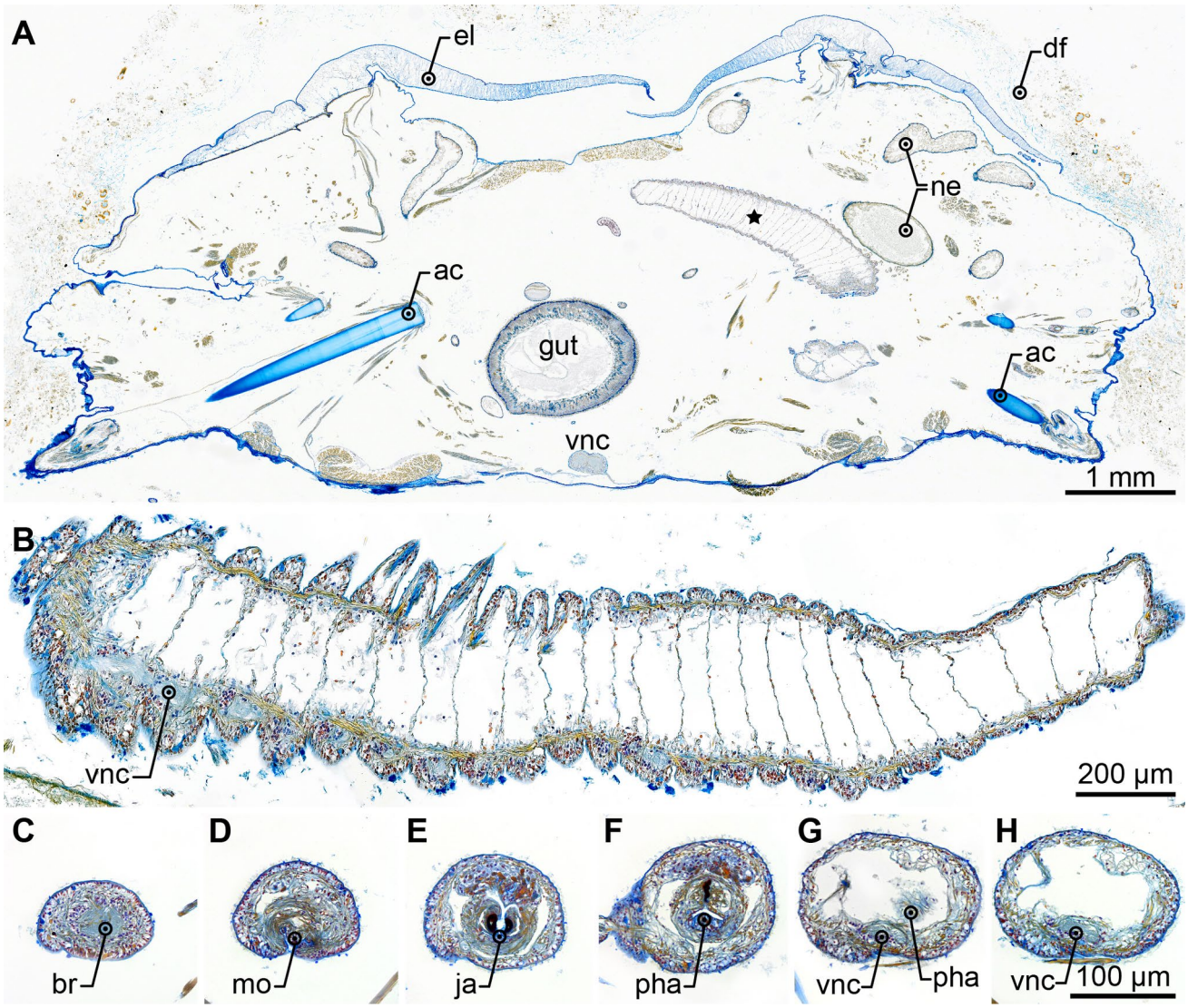

Fig. 4 AZAN-stained paraffin histology. **A** Histological cross-section of a juvenile *Aphrodita longipalpa* featuring an endoparasitic immature *Veneriserva pygoclava* (denoted by a star). **B** Longitudinal section of *V. pygoclava*, highlighting the absence of a through gut, and continuous uninterrupted mesenteries. **C–H** Cross-sections through the anterior region of *V. pygoclava*, showing the muscularized pharynx with jaws culminating in blind termination at section **G**. Abbreviations—*ac* acicula, *br* brain, *df* dorsal felt, *el* elytra, *ja* jaws, *mo* mouth, *ne* nephridium, *pha* pharynx, *vnc* ventral nerve cord

the cuticle (Fig. 6A–C). The cuticle was less than 500 µm in thickness. A thin electron-dense epicuticle was present and had an inner lighter and an outer denser zone. The outer electron dense zone of the epicuticle was covered with a thin layer of darkly stained particles, giving it a fuzzy appearance (Fig. 6B). The unbanded collagen fibers of the cuticle were embedded in an electron-light glycocalyx matrix and were more densely arranged towards the epicuticle (Fig. 6B). Distally, the epidermal cells contained numerous transport vesicles (inclusion bodies) (Fig. 6E). Individual mucosecretory cells were abundant in the epidermis and were situated between supportive cells (Fig. 6A). Patches of multiciliated epidermal cells were present scattered around the body (Fig. 6D). These multiciliated cells contained larger amounts of mitochondria and were also covered with microvilli (Fig. 6D). Microvilli were branched (Fig. 6E) and had an enlarged, inflated tip covered with electron-dense droplets (Fig. 6B). The inflated portion of a microvillus was bulbous and had a maximum diameter of ± 300 nm.

Phylogenetic placement of *Veneriserva*

The ML analysis of the three mitochondrial and two nuclear genes for Dorvilleidae showed two main clades (labeled A and B) containing all *Ophryotrocha* terminals as well as members of other genera such as *Exallopus*, *Iphitime*,

Pseudophryotrocha, and *Veneriserva*. *Veneriserva pygoclava* was in clade B with a relatively long branch and formed a poorly supported clade with the three included terminals of *Iphitime* (Fig. 7), which are all symbiotic with Crustacea (de Paiva and Nonato, 1991). It was sister taxon to *Iphitime paguri* Fage & Legendre, 1934, making *Iphitime* paraphyletic, though there was little support for this. This *Iphitime*/*Veneriserva* clade formed a well-supported clade together with a sister clade of *Ophryotrocha* mainly associated with hydrothermal vents (6 species) (Zhang et al., 2023) and one with a whale fall *O. clava* Taboada et al., 2013. Another clade of symbiotic dorvilleids, also living with Crustacea (*O. mediterranea* Martin et al., 1991 and *O. geryonicola* Esmark, 1874), formed a clade with the free-living *O. vivipara* Banse, 1963 (Fig. 7) and was also in clade B. Five specimens of *V. pygoclava* exhibited four CO1 haplotypes, each differing by a few mutational steps (Fig. 7).

Mitochondrial genome of *Veneriserva pygoclava*

The mitochondrial genome of *Veneriserva pygoclava* was found to span a length of 15,709 base pairs (bp) (Fig. 8). The GC content is measured at 27.4%. In our analysis, we have successfully identified a total of 13 protein-coding genes (cox1, cox2, cox3, nad1, nad2, nad3, nad4, nad4l, nad5, nad6, cytb, atp6, and atp8), accompanied by two rRNAs and a set of 22 tRNAs. The arrangement of these mitochondrial genes presents a deviation from the typical pattern observed in the majority of annelids.

Discussion

Host infection

Our analysis of *Aphrodita longipalpa* specimens suggests that the infection rate of *Veneriserva pygoclava* is relatively high in the San Diego area. At least 64%, over the various sets of samples taken through most of the year. A study by Micaletto et al. (2002) examined the infection rate of the Antarctic subspecies *V. pygoclava meridionalis* in another aphroditid, *Laetmonice producta* and found an infection rate of approximately 20% in their analysis of 842 host specimens. To our knowledge *Veneriserva* specimens have not been reported in any other location thus far. The two juvenile *Aphrodita* specimens that we sectioned histologically both had a single juvenile parasite. These were not visible upon external examination of the hosts. This suggests that the penetration of the hosts occurs very early during the host development and demonstrates that small *Veneriserva* specimens can be easily overlooked upon initial examination. *Veneriserva pygoclava* specimens evidently mature within the coelomic cavity of the hosts and most likely never leave their host once settled, as they lack a functional gut (see below for more details). However, the specific mechanism of host entry remains unclear. We hypothesize that the larval stages of the parasite are sufficiently small to enter and exit the coelomic cavity of *A. longipalpa* through its nephridia (Figs. 3B, C and 4A).

The parasitization of a single host by multiple individuals of *Veneriserva* had been previously reported (Micaletto et al., 2002; Rossi, 1984). Rossi (1984) in his original description mentions four specimens collected from a single host. The highest amount of *Veneriserva* reported from a single host was six in Micaletto et al. (2002). In our study, we never found more than three parasites within a single *Aphrodita* specimen. Interestingly, neither Rossi (1984) nor Micaletto et al. (2002) and Micaletto et al. (2003) report finding male *Veneriserva*. Rossi (1984) only identifies the largest specimen, which is the holotype, as a female and does not comment on the sex of the paratypes, while Micaletto et al. (2002) did not find any males and only report female *Veneriserva* that they were able to recognize by the presence of large eggs.

We now, for the first time, report the presence of male and female *Veneriserva* within a single host. Males are much smaller than females and easier to be overlooked. Furthermore, spermatozoa in these small individuals are less conspicuous making it more challenging to determine the sex of male *Veneriserva* without comprehensive morphological investigation. Therefore, it is likely that both Rossi (1984) and Micaletto et al. (2002) also had male *Veneriserva* in their samples. We never found any of the host *A. longipalpa* with gametes, although they were sampled over much of the year. Micaletto et al. (2003) found no evidence for an impact of *V. pygoclava meridionalis* on reproduction of its host *L. producta*, which appears to breed constantly throughout the year. Little is known about reproduction in Aphroditidae otherwise.

Reproductive strategy of *Veneriserva*

The presence of male and female *Veneriserva pygoclava* within the same host also may indicate that the parasites reproduce within the coelomic cavity of the host. Considering the large number of eggs produced by female *Veneriserva pygoclava*, the most plausible reproductive strategy seems to be that mature oocytes and spermatozoa are released into the coelomic cavity of the host and fertilized therein. Thereby, the body cavity of *Aphrodita* may be used almost like a brood chamber, increasing the chance of successful fertilization of eggs by providing a contained and protected space. The sperm morphology provides further support for this hypothesis. Sperm morphology (though not without exceptions) can be correlated to the fertilization mechanism (Franzen, 1956; Rouse, 2005). The sperm of

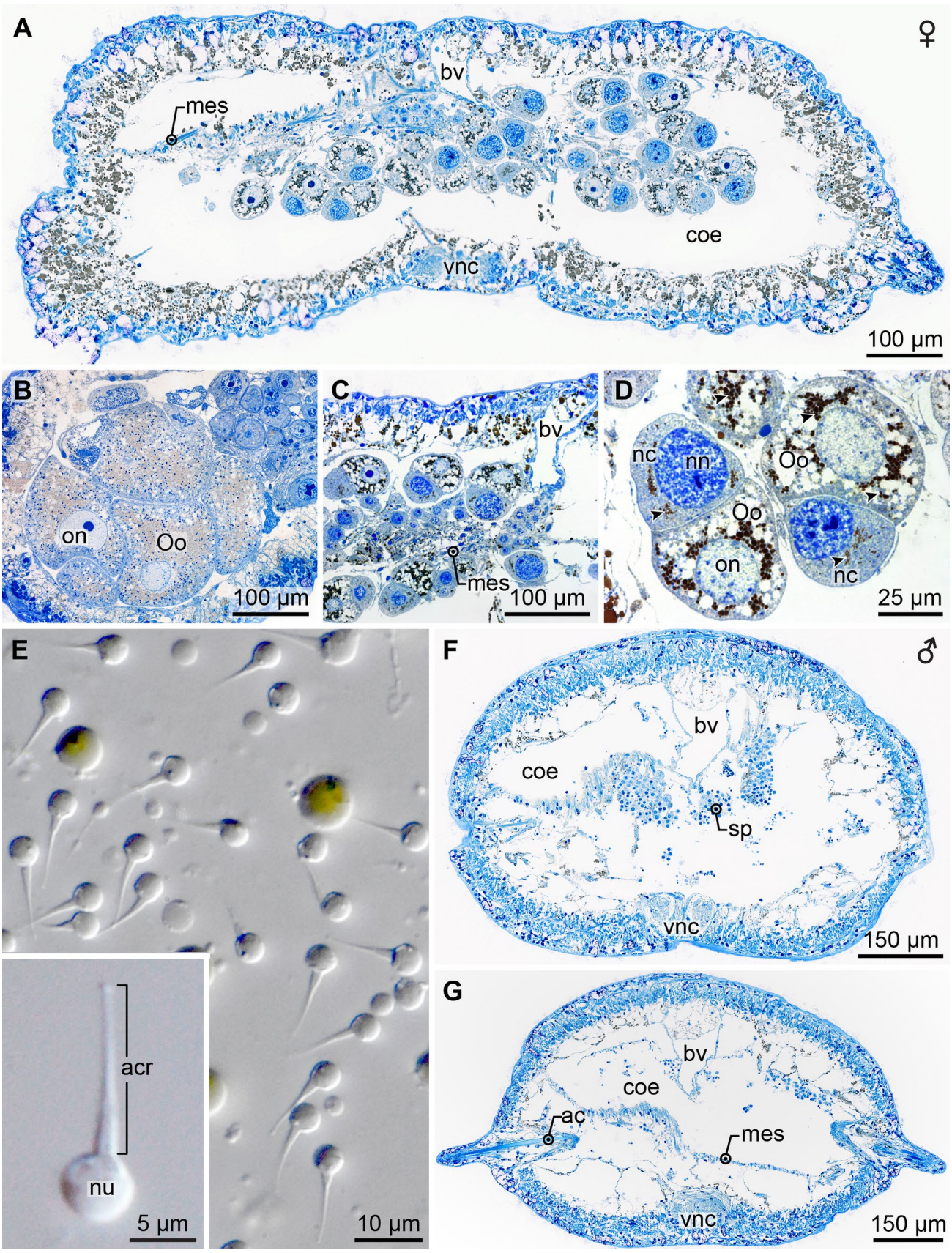
A
♀
bv
mes
coe
vnc
100 µm
B
on
Oo
100 µm
C
bv
mes
100 µm
D
nc
nn
Oo
Oo
on
nc
25 µm
E
acr
nu
5 µm
10 µm
F
♂
bv
coe
sp
vnc
150 µm
G
bv
coe
ac
mes
vnc
150 µm

◂**Fig. 5** Gametogenesis in male and female *Veneriserva pygoclava*. **A**–**D** Semi-thin histological sections of female *Veneriserva pygoclava*, stained with toluidine blue. **A** Cross-section of a female *Veneriserva*. **B** Close-up of large mature oocytes without discernible nurse cells. **C** Developing oocytes attached to mesenteries (*mes*), and oogonia proliferating from the ventral side of the dorsal blood vessel (*bv*). **D** Details of vitellogenic oocytes and nurse cells. Arrowheads indicate brown-stained yolk platelets and yolk bodies. **E** Live sperm cells captured in a light micrograph. **F**–**G** Cross-sections of male *Veneriserva*. Note the absence of a gut in the cross-sections. Abbreviations—*ac* acicula, *acr* acrosome, *bv* blood vessel, *coe* coelomic cavity, *mes* mesentery, *nc* nurse cell, *nn* nurse cell nucleus, *nu* sperm cell nucleus, *Oo* oocyte, *on* oocyte nucleus, *sp* spermatogonia, *vnc* ventral nerve cord

Ophryotrocha lack long flagella, making pseudocopulation a prerequisite for successful fertilization in a cocoon (Berruti et al., 1978; Troyer & Schwager, 1979). The sperm of *Veneriserva* is similar to that of *Ophryotrocha* and suggests that fertilization occurs without the spermatozoa having to swim a long distance.

Micaletto et al. (2002) proposed that some specimens of *V. pygoclava meridionalis* were regenerating and speculated that asexual reproduction, as well as sexual reproduction, might be occurring in this species. We did not observe any regenerating specimens. It is possible that the observation of Micaletto et al. (2002) might be explained by the fact that the pygidium is significantly elongated in *V. pygoclava meridionalis* making the posterior end of the animal resemble a regenerative bud. Asexual reproduction by budding is not known for any Dorvilleidae, and it is highly unlikely that the parasites would have wounded posterior ends within the protected body cavity of the host. Considering all this and our findings showing the cohabitation of both sexes, sexual reproduction seems to be the primary reproductive strategy in *Veneriserva*.

Epidermal nutrient uptake in *Veneriserva*

One unanticipated finding in our study was the complete reduction of a digestive tract in both adult and juvenile specimens of *Veneriserva pygoclava*. This observation indicates that the reduction of the gut happens early during development. Currently, there is no information available about the post-embryonic development in *V. pygoclava.* Future developmental studies could not only elucidate the ontogenetic process leading to gut reduction but could also shed light on critical aspects of *V. pygoclava*'s biology, such as larval dispersal, mechanisms, and strategies for host penetration.

Gutless annelids are known, but rare and so far, had been restricted to deep-sea Siboglinidae that rely on symbiotic bacteria for their nutrition (Cavanaugh et al., 1981; Goffredi et al., 2005), to phallodrilin oligochaetes also living with bacterial symbionts (Dubilier et al., 2006; Erseus, 1984) and to the interstitial polychaete *Astomus taenioides* Jouin, 1979 (Martínez et al., 2015). In *A. taenioides*, there are no bacterial symbionts, the animals lack a mouth opening, and a non-functional residual gut is present. In the case of these meiofaunal polychaetes, the nutrients appear to come in the form of dissolved and particulate organic matter, possibly from the detritus in the sediment that the animals dwell in. However, the origin and nature of their nutritional source still remains unresolved (Jouin, 1992).

In the undoubtedly endoparasitic *V. pygoclava*, however, the nutrients must stem from the coelomic fluid of the host. In contrast to *A. taenioides*, *V. pygoclava* has a mouth opening and a functional muscular axial proboscis with distinct jaws. There is no vestigial gut and the pharynx ends blindly. It is possible, therefore, that the jaws play a role in moving/biting through the host's tissues, although no significant damage to the host's internal organs or musculature was observed. The enlarged epidermal surface area, with elongated microvilli covering the entire body and extending over the thin cuticle, is likely to play an active role in the transport of dissolved organic compounds from the coelomic fluid of the host. Ciliated patches along the body may be agitating the microenvironment around the parasite to enhance the flux of coelomic fluid and thereby of nutrients along the epidermal surface. The presence of numerous subcuticular transport vesicles in the supportive cells of the epidermis indicates that particulate organic matter is taken up through endocytosis and digested in the epidermis. The integument of an endoparasitic animal is the direct interface between the parasite and the host, and thus plays a crucial role in both defense against the host's immune system, as well as in nutrient acquisition, as described above. A similar mechanism of nutrient uptake is best-known from gutless endoparasitic tapeworms (Dalton et al., 2004; Poddubnaya et al., 2007; Tyler & Hooge, 2004). The epidermis, or tegument, of a tapeworm is syncytial, with its surface area significantly increased by dense surface projections forming a "tegument brush" (Lumsden, 1975), although the microvilli covering the apical surface of the epidermis are not as densely arranged or as elongated as the "microtriches"—the digitiform projections of the neodermis in tapeworms. In *V. pygoclava*, the epidermal microvilli likely serve to expand the surface area for nutrient absorption. In contrast, tapeworm microvilli also play a crucial role in maintaining a high-pH boundary layer, which protects against digestion by the host's intestinal enzymes (Tyler & Hooge, 2004). However, since *V. pygoclava* resides in the coelom rather than the gut, this protective function is less likely to be applicable. *V. pygoclava* is the only known obligate endoparasitic annelid with the ability to absorb particulate material and nutrients from the ambient milieu through its epidermis.

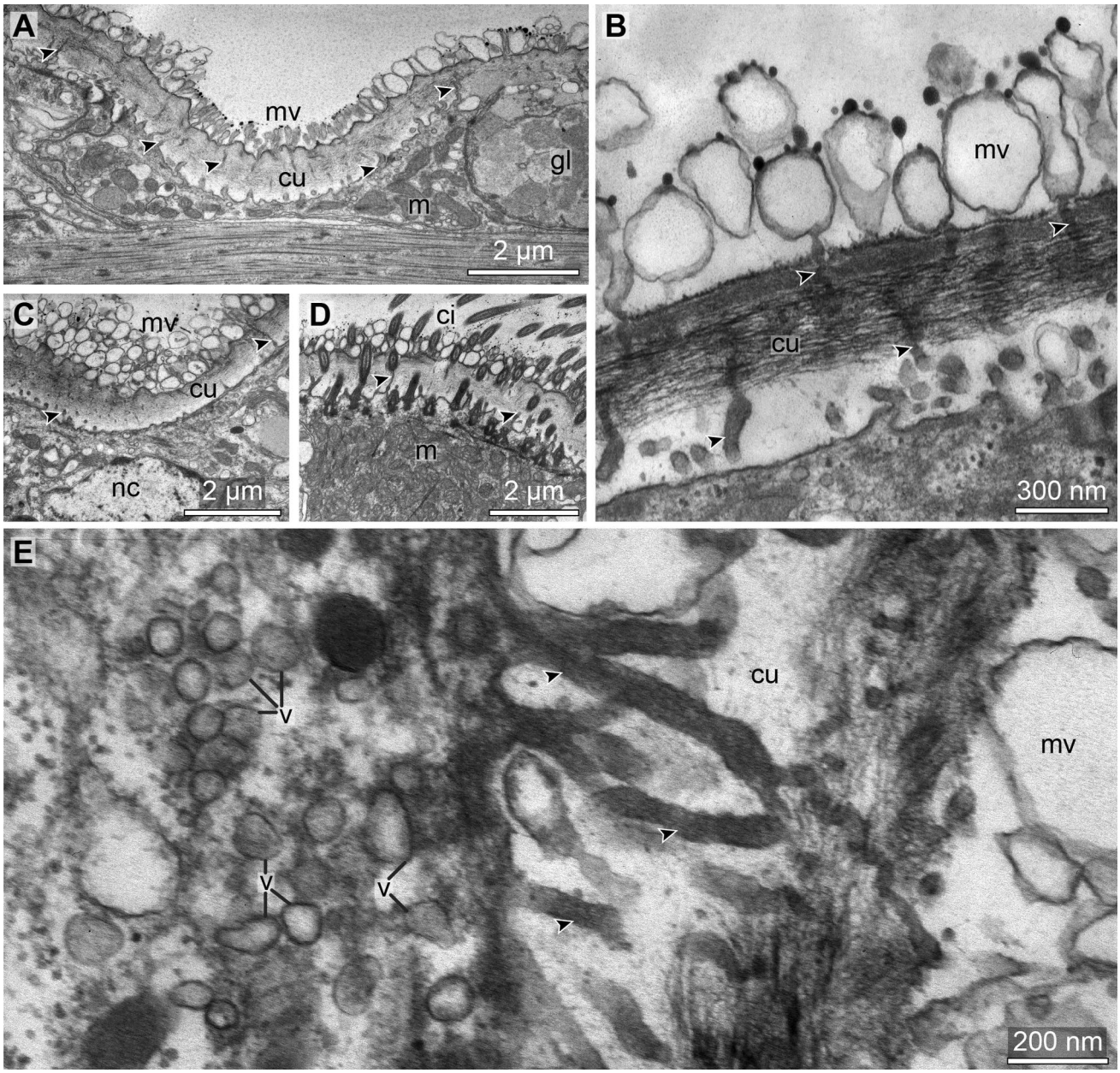

Fig. 6 Epidermal ultrastructure of *Veneriserva pygoclava*. **A**–**D** TEM images of the epidermis revealing the presence of dense, modified microvilli (*mv*) that cover the body surface. A mucosecretory gland cell (*gl*) is discernable in **A**. **D** shows details of a multi-ciliated epidermal cell. **B** depicts the microvilli (*mv*) covering the cuticle (*cu*). Note the inflated tips of the microvilli and the electron-dense droplets. **E** Apically the epidermal cells display an abundance of transport vesicles (*v*). Arrowheads mark the branching microvilli piercing through the cuticle in all images. Abbreviations—*ci* cilia, *m* mitochondria, *nc* nucleus

Phylogenetic placement of *Veneriserva*

Veneriserva pygoclava was recovered well inside the genus *Ophryotrocha*, which has been acknowledged as a paraphyletic group for some time (see Zhang et al., 2023). What was more striking was that *Veneriserva* was also nested within the genus *Iphitime*, which was represented by three terminals in Fig. 7. Other *Iphitime* species were not used in the analysis, including the type species, *Iphitime doederleini* Marenzeller, 1902, which prevents us from taking any taxonomical action regarding the synonymization of genera *Iphitime* and *Veneriserva*. In addition, we noted here the sister group relationship of *O. puerilis* with *O. eutrophila* and with what has normally (Bacci & La Greca, 1953) been regarded as *O. puerilis siberti* as the sister group to this clade (Fig. 7). There seems

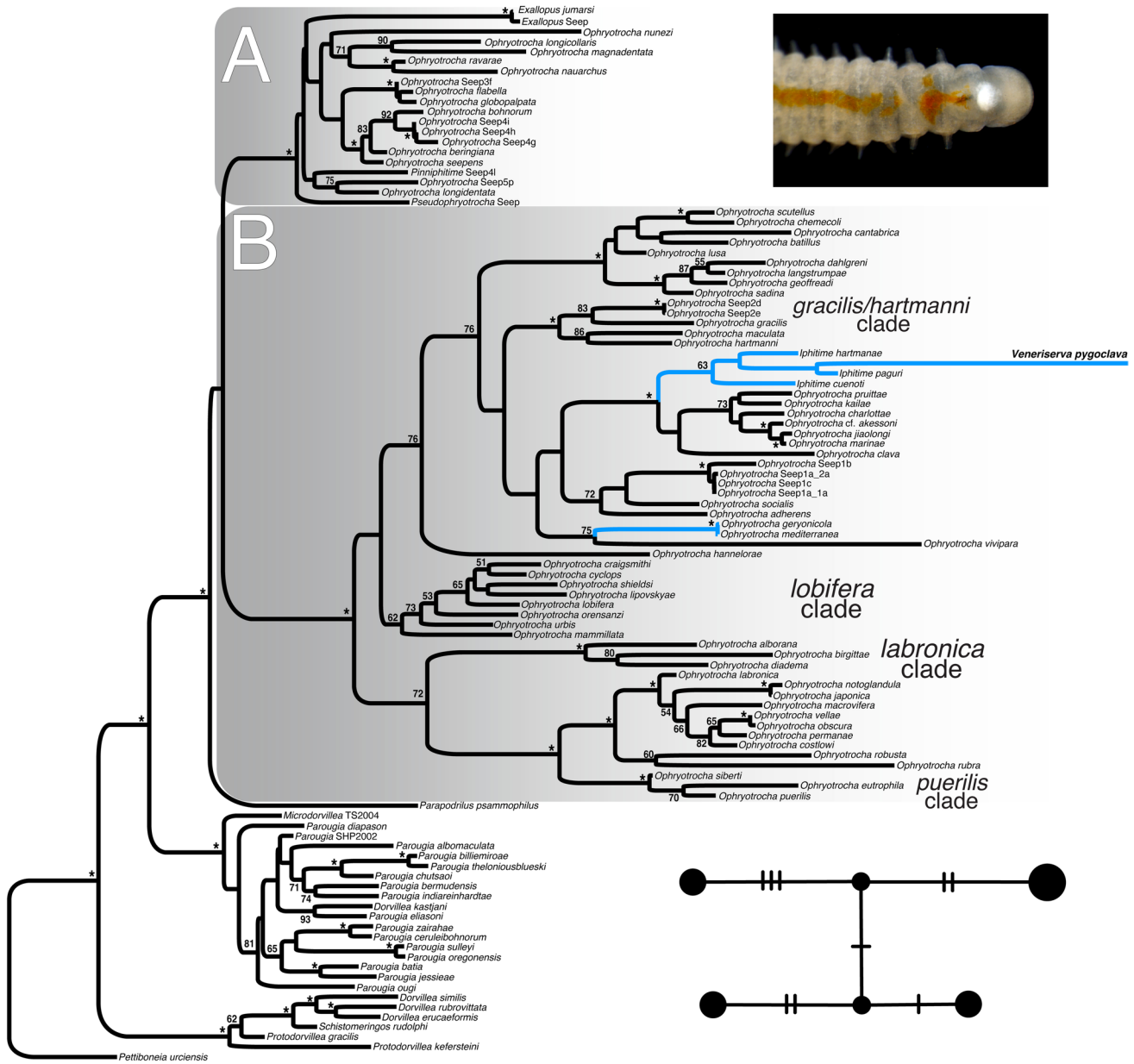

Fig. 7 Maximum likelihood (ML) tree of Dorvilleidae. The tree depicts the phylogenetic relationships within Dorvilleidae inferred through concatenated 16S, COI, Cytb, 18S, and H3 sequences. Bootstrap support values are provided for each node. Nodes with complete support are indicated with an asterisk (*); values below 50% are not shown. Branches of parasitic/symbiotic species highlighted in blue. Haplotype network for 5 *Veneriserva pygoclava* specimens is shown next to the tree

to be no justification for regarding *O. siberti* as a subspecies of *O. puerilis*, especially given its nearly 20% COI divergence so we have labeled it in Fig. 7 as *O. siberti* and formally restore to species rank. These two species, currently regarded as subspecies, were originally described from two different localities: Whitstable and Plymouth in the Atlantic (*Staurocephalus siberti*, McIntosh, 1885) and the Bay of Naples in the Mediterranean (*Ophryotrocha puerilis*, Claparède & Mecznikow, 1869). Later, Fauvel (1923) synonymized *S. siberti* with *O. puerilis*. Bacci and La Greca (1953) subsequently treated McIntosh's species as a subspecies of *O. puerilis* despite finding clear morphological differences in the mandibles. More recently, Paxton and Åkesson (2007) presented a formal taxonomy for *Ophryotrocha puerilis siberti*. However, despite reporting again clear morphological differences in the mandibles and very low success in hybridization, they kept *O. puerilis siberti* at subspecies rank (Paxton & Åkesson, 2007). In 2009, Wiklund et al. (2009) presented molecular data from three genes and including *O. puerilis puerilis* and

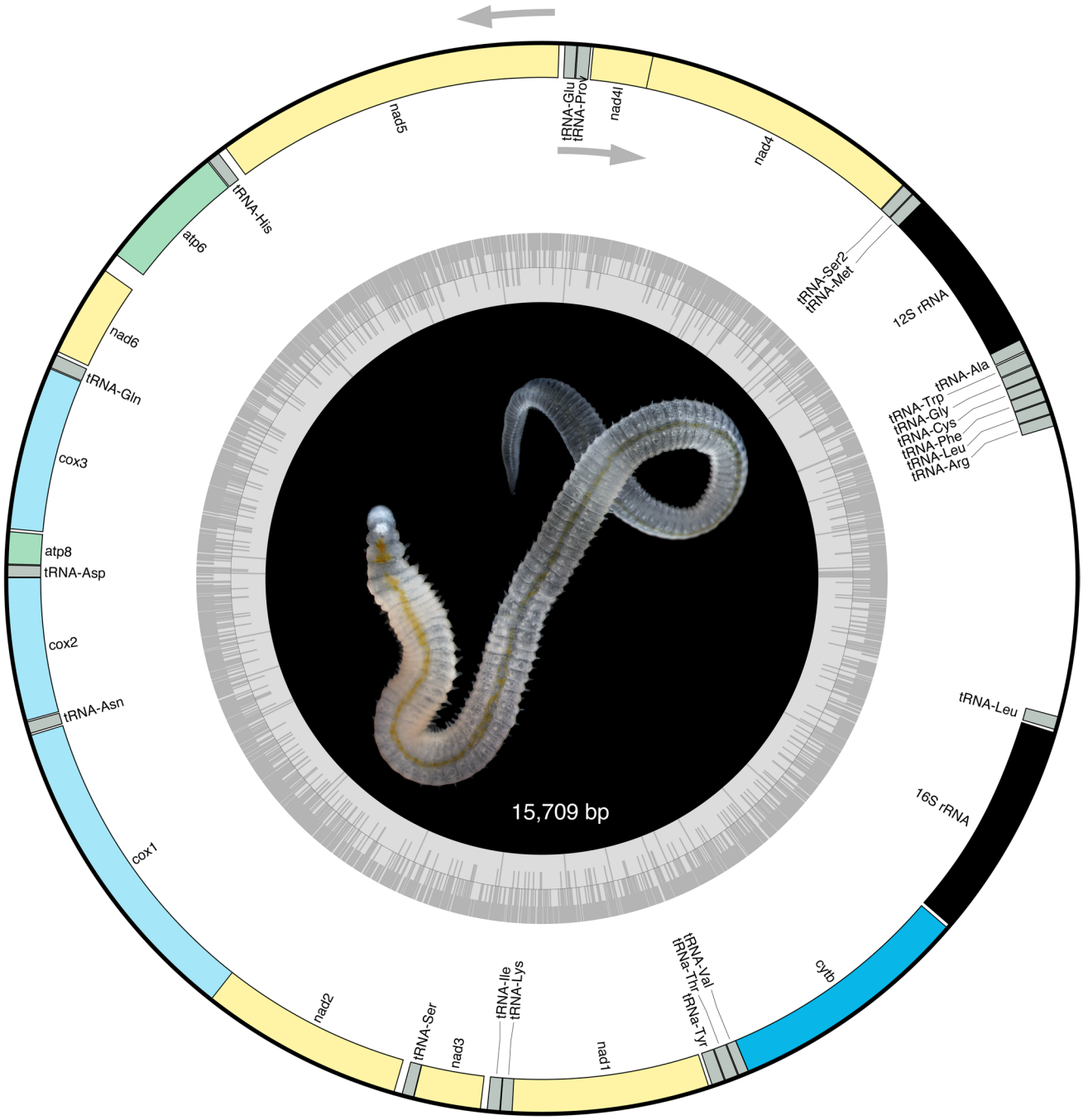

Fig. 8 Mitochondrial genome map of *Veneriserva pygoclava*. The inner ring presents the GC content graph. The complete, fully annotated mitochondrial genome is accessible via the NCBI GenBank database under the accession number: OR449961

O. puerilis siberti, recovering them as sister taxa, though with branch length differences that were greater than those between sister species pairs on the same tree, however no taxonomic action was taken. Our analysis here, with five genes instead of three (Fig. 7), shows *O. puerilis siberti* is not the sister taxon to *O. puerilis puerilis*. Also, the COI distance between these two taxa is nearly 20%. For all these reasons, we now suggest to formally give the status of species to *Ophryotrocha puerilis* Claparède & Mecznikow, 1869 (previously considered as *O. puerilis puerilis*) and to *Ophryotrocha siberti* (McIntosh, 1885) (previously considered as *O. puerilis siberti*).

Mitochondrial gene rearrangements in *Veneriserva*

Recent studies have highlighted the mostly conserved nature of mitochondrial gene order in annelids (Struck et al., 2023; Weigert et al., 2016). Despite this predominantly conserved pattern, various exceptions have been documented, revealing deviations from the presumed standard mitochondrial gene order (Aguado et al., 2016; Alves et al., 2020; Seixas et al., 2017; Sun et al., 2021; Tempestini et al., 2020; Zhang et al., 2018). Furthermore, certain taxa exhibit considerable variability, even within a single genus. For example, species within *Hydroides* (Serpulidae) (Sun et al., 2021) and *Ophryotrocha* (Dorvilleidae) (Tempestini et al., 2020) display extensive rearrangements.

The mitochondrial gene order in *V. pygoclava* significantly departs from the patterns observed in previously published annelid mitogenomes. However, considering *Veneriserva*'s placement nested within *Ophryotrocha* and the documented variability of mitogenomes within this group (Tempestini et al., 2020), this divergence is not unexpected. Tempestini et al. (2020) based their analyses on six *Ophryotrocha* species (*O. puerilis*, *O. robusta*, *O. japonica*, *O. labronica*, *O. diadema*, and *O. adherens*), predominantly from the *labronica/puerilis* clade (Fig. 7, clade B), to which *Veneriserva* also belongs. Sampling more distantly related *Ophryotrocha* species is likely to unveil even more distinct gene arrangement patterns.

Parasitism has been proposed as a potential biological factor driving mitochondrial gene rearrangements (Bernt et al., 2013); this hypothesis did not receive statistical confirmation within annelids in the recent study by Struck et al. (2023). Nevertheless, the complete rearrangement of the mitochondrial genome in *Veneriserva* remains intriguing, albeit not entirely unexpected.

Supplementary Information The online version contains supplementary material available at https://doi.org/10.1007/s13127-023-00633-8.

Acknowledgements The specimens of *Aphrodita longipalpa* (and so *Veneriserva pygoclava*) were all collected on undergraduate and graduate student cruises funded by the University of California ship funds. We thank Phil Zerofski for putting aside live specimens on several occasions for this study. We would like to thank Christiane Wallnisch, who sectioned the material for paraffin histology. The µCT scanner was funded by the State of North Rhine-Westphalia and the German Research Foundation (DFG) — *INST 217/849-1 FUGG*. We thank Dr. Alexander Ziegler for his help with the µCT scan. Many thanks also to Dr. Charlotte Seid and to Marie-Louise Tritz for organizing the shipment of specimens and cataloging vouchers at the Benthic Invertebrate Collection of Scripps Institution of Oceanography (SIO-BIC) and at the Marine Invertebrates II collection of the Senckenberg Natural History Museum, Frankfurt (SMF).

Funding Open Access funding enabled and organized by Projekt DEAL.

Data availability The datasets generated during and/or analyzed during the current study are available freely in the online repositories. All sequence data is uploaded to NCBI GenBank. The entire µCT dataset is published together with this paper and is available under https://doi.org/10.5281/zenodo.8260723.

Declarations

Competing interests The authors declare no competing interests.

References

Aguado, M. T., Richter, S., Sontowski, R., Golombek, A., Struck, T. H., & Bleidorn, C. (2016). Syllidae mitochondrial gene order is unusually variable for Annelida. *Gene, 594*(1), 89–96. https://doi.org/10.1016/j.gene.2016.08.050

Alves, P. R., Halanych, K. M., & Santos, C. S. G. (2020). The phylogeny of Nereididae (Annelida) based on mitochondrial genomes. *Zoologica Scripta, 49*(3), 366–378. https://doi.org/10.1111/zsc.12413

Bacci, G., & La Greca, M. (1953). Genetic and morphological evidence for subspecific differences between Naples and Plymouth populations of *Ophryotrocha puerilis*. *Nature, 171*(4364), 1115. https://doi.org/10.1038/1711115a0

Bankevich, A., Nurk, S., Antipov, D., Gurevich, A. A., Dvorkin, M., Kulikov, A. S., Lesin, V. M., Nikolenko, S. I., Pham, S., Prjibelski, A. D., & Pyshkin, A. V. (2012). SPAdes: A new genome assembly algorithm and its applications to single-cell sequencing. *Journal of Computational Biology: A Journal of Computational Molecular Cell Biology, 19*(5), 455–477. https://doi.org/10.1089/cmb.2012.0021

Banse, K. (1963). Polychaetous annelids from Puget Sound and the San Juan Archipelago, Washington. *Proceedings of the Biological Society of Washington, 76*, 197–208.

Bernt, M., Bleidorn, C., Braband, A., Dambach, J., Donath, A., Fritzsch, G., Golombek, A., Hadrys, H., Jühling, F., Meusemann, K., & Middendorf, M. (2013). A comprehensive analysis of bilaterian mitochondrial genomes and phylogeny. *Molecular Phylogenetics and Evolution, 69*(2), 352–364. https://doi.org/10.1016/j.ympev.2013.05.002

Berruti, G., Ferraguti, M., & Donin, C. L. L. (1978). The aflagellate spermatozoon of *Ophryotrocha*: A line of evolution of fertilization among polychaetes. *Gamete Research, 1*(3–4), 287–292. https://doi.org/10.1002/mrd.1120010309

Blumer, M. J. F., Gahleitner, P., Narzt, T., Handl, C., & Ruthensteiner, B. (2002). Ribbons of semithin sections: An advanced method with a new type of diamond knife. *Journal of Neuroscience Methods, 120*(1), 11–16. https://doi.org/10.1016/S0165-0270(02)00166-8

Cavanaugh, C. M., Gardiner, S. L., Jones, M. L., Jannasch, H. W., & Waterbury, J. B. (1981). Prokaryotic cells in the hydrothermal vent tube worm *Riftia pachyptila* Jones: Possible chemoautotrophic symbionts. *Science, 213*(4505), 340–342. https://doi.org/10.1126/science.213.4505.340

Claparède, É., & Mecznikow, E. (1869). Beiträge zur Kenntnis der Entwicklungsgeschichte der Chaetopoden. *Zeitschrift für wissenschaftliche Zoologie*, 163–205.

Dalton, J. P., Skelly, P., & Halton, D. W. (2004). Role of the tegument and gut in nutrient uptake by parasitic platyhelminths. *Canadian Journal of Zoology, 82*(2), 211–232. https://doi.org/10.1139/z03-213

Darriba, D., Posada, D., Kozlov, A. M., Stamatakis, A., Morel, B., & Flouri, T. (2020). ModelTest-NG: A new and scalable tool for the selection of DNA and protein evolutionary models. *Molecular Biology and Evolution, 37*(1), 291–294. https://doi.org/10.1093/molbev/msz189

de Paiva, P. C., & Nonato, E. F. (1991). On the genus *Iphitime* (Polychaeta: Iphitimidae) and description of *Iphitime sartorae* sp. nov. a commensal of brachyuran crabs. *Ophelia*, *34*(3), 209–215. https://doi.org/10.1080/00785326.1991.10429696

Donath, A., Jühling, F., Al-Arab, M., Bernhart, S. H., Reinhardt, F., Stadler, P. F., Middendorf, M., & Bernt, M. (2019). Improved annotation of protein-coding genes boundaries in metazoan mitochondrial genomes. *Nucleic Acids Research, 47*(20), 10543–10552. https://doi.org/10.1093/nar/gkz833

Dubilier, N., Blazejak, A., & Rühland, C. (2006). Symbioses between bacteria and gutless marine oligochaetes. *Progress in Molecular and Subcellular Biology, 41*, 251–275. https://doi.org/10.1007/3-540-28221-1_12

Edler, D., Klein, J., Antonelli, A., & Silvestro, D. (2021). raxmlGUI 2.0: A graphical interface and toolkit for phylogenetic analyses using RAxML. *Methods in ecology and evolution / British Ecological Society*, *12*(2), 373–377. https://doi.org/10.1111/2041-210x.13512

Emerson, R. R. (1974). A new species of polychaetous annelid (Arabellidae) parasitic in *Diopatra ornata* (Onuphidae) from southern California. *Bulletin of the Southern California Academy of Sciences, 73*(1), 1–5.

Erseus, C. (1984). Taxonomy and phylogeny of the gutless Phallodrilinae (Oligochaeta, Tubificidae), with descriptions of one new genus and twenty-two new species. *Zoologica Scripta, 13*(4), 239–272. https://doi.org/10.1111/j.1463-6409.1984.tb00041.x

Esmark, L. (1874). Forhandlinger fra Videnskabs-Selskabet i Christiania. 497–498.

Essenberg, C. (1917). On some new species of Aphroditidae from the coast of California. *University of California Publications in Zoology, 16*(22), 401–430.

Fage, L., & Legendre, R. (1934). Les annélides polychètes du genre *Iphitime*. A propos d'une espece nouvelle commensale des pagures, *Iphitime paguri* n.sp. *Bulletin De La Société Zoologique De France, 58*, 299–305.

Fauvel, P. (1923). Polychètes errantes. Faune de France. Librairie de la Faculte des Sciences. *Paris., 5*, 1–488.

Franzen, A. (1956). On spermiogenesis, morphology of the spermatozoon, and biology of fertilization among invertebrates. *Zool Bidrag, Uppsala, 31*, 355–482.

Goffredi, S. K., Orphan, V. J., Rouse, G. W., Jahnke, L., Embaye, T., Turk, K., Lee, R., & Vrijenhoek, R. C. (2005). Evolutionary innovation: A bone-eating marine symbiosis. *Environmental Microbiology, 7*(9), 1369–1378. https://doi.org/10.1111/j.1462-2920.2005.00824.x

Hernández-Alcántara, P., & Solís-Weiss, V. (1998). Parasitism among polychaetes: A rare case illustrated by a new species: *Labrorostratus zaragozensis*, n. sp. (Oenonidae) found in the Gulf of California, Mexico. *The Journal of parasitology*, *84*(5), 978–982. https://doi.org/10.2307/3284631

Jimi, N., Kimura, T., Ogawa, A., & Kajihara, H. (2021). Alien worm in worm: A new genus of endoparasitic polychaete (Phyllodocidae, Annelida) from scale worms (Aphroditidae and Polynoidae, Annelida). *Systematics and Biodiversity, 19*(1), 13–21. https://doi.org/10.1080/14772000.2020.1785038

Jin, J.-J., Yu, W.-B., Yang, J.-B., Song, Y., dePamphilis, C. W., Yi, T.-S., & Li, D.-Z. (2020). GetOrganelle: A fast and versatile toolkit for accurate de novo assembly of organelle genomes. *Genome Biology, 21*(1), 241. https://doi.org/10.1186/s13059-020-02154-5

Jouin, C. (1979). Description of a free-living polychaete without gut: *Astomus taenioides* n.gen., n.sp. (Protodrilidae, Archiannnelida). *Canadian Journal of Zoology*, *57*(12), 2448–2456

Jouin, C. (1992). The ultrastructure of a gutless annelid, *Parenterodrilus* gen. nov. *taenioides* (= *Astomus taenioides*) (Polychaeta, Protodrilidae). *Canadian journal of zoology*, *70*(9), 1833–1848. https://doi.org/10.1139/z92-250

Katoh, K., & Standley, D. M. (2013). MAFFT multiple sequence alignment software version 7: Improvements in performance and usability. *Molecular Biology and Evolution, 30*(4), 772–780. https://doi.org/10.1093/molbev/mst010

Kozlov, A., Darriba, D., Flouri, T., Morel, B., & Stamatakis, A. (2019). RAxML-NG: A fast, scalable, and user-friendly tool for maximum likelihood phylogenetic inference. *Bioinformatics, 35*(21), 4453–4455. https://doi.org/10.1093/bioinformatics/btz305

Langmead, B., & Salzberg, S. L. (2012). Fast gapped-read alignment with Bowtie 2. *Nature Methods, 9*(4), 357–359. https://doi.org/10.1038/nmeth.1923

Leigh, J. W., & Bryant, D. (2015). POPART: Full-feature software for haplotype network construction. *Methods in Ecology and Evolution, 6*(9), 1110–1116. https://doi.org/10.1111/2041-210X.12410

Limaye, A. (2012). Drishti: A volume exploration and presentation tool. In *Developments in X-ray tomography VIII* (Vol. 8506, pp. 191–199). Presented at the Developments in X-Ray Tomography VIII, SPIE. https://doi.org/10.1117/12.935640

Lohse, M., Drechsel, O., & Bock, R. (2007). OrganellarGenomeDRAW (OGDRAW): A tool for the easy generation of high-quality custom graphical maps of plastid and mitochondrial genomes. *Current Genetics, 52*(5–6), 267–274. https://doi.org/10.1007/s00294-007-0161-y

Lumsden, R. D. (1975). Surface ultrastructure and cytochemistry of parasitic helminths. *Experimental Parasitology, 37*(2), 267–339. https://doi.org/10.1016/0014-4894(75)90078-8

Martin, D., Abelló, P., & Cartes, J. (1991). A new species of *Ophryotrocha* (Polychaeta: Dorvilleidae) commensal in *Geryon longipes* (Crustacea: Brachyura) from the western Mediterranean Sea. *Journal of Natural History, 25*(2), 279–292. https://doi.org/10.1080/00222939100770201

Martin, D., & Britayev, T. A. (1998). Symbiotic polychaetes: Review of known species. *Oceanography and Marine Biology: An Annual Review, 36*, 217–340.

Martin, D., & Britayev, T. A. (2018). Symbiotic polychaetes revisited: An update of the known species and relationships (1998–2017). *Oceanography and Marine Biology*. https://doi.org/10.1201/9780429454455-6

Martínez, A., Di Domenico, M., Rouse, G. W., & Worsaae, K. (2015). Phylogeny and systematics of Protodrilidae (Annelida) inferred with total evidence analyses. *Cladistics: the international journal of the Willi Hennig Society*, *31*(3), 250–276. https://doi.org/10.1111/cla.12089

McIntosh, W. C. (1885). Notes from the St. Andrews Marine Laboratory (under the Fishery Board for Scotland). No. III. 2. On a new British Staurocephalus. *The Annals and Magazine of Natural History, including Zoology, Botany and Geology. Series 5, 16*(96), 480–487.

Metscher, B. D. (2009). MicroCT for comparative morphology: Simple staining methods allow high-contrast 3D imaging of diverse non-mineralized animal tissues. *BMC Physiology, 9*, 11. https://doi.org/10.1186/1472-6793-9-11

Micaletto, G., Gambi, M. C. & Cantone, G. (2002). A new record of the endosymbiont polychaete *Veneriserva* (Dorvilleidae), with description of a new sub-species, and relationships with its host *Laetmonice producta* (Polychaeta: Aphroditidae) in Southern Ocean waters (Antarctica). *Marine Biology, 141*(4), 691–698. https://doi.org/10.1007/s00227-002-0870-1

Micaletto, G., Gambi, M. C., & Piraino, S. (2003). Observations on population structure and reproductive features of *Laetmonice producta* Grube (Polychaeta, Aphroditidae) in Antarctic waters. *Polar Biology, 26*(5), 327–333. https://doi.org/10.1007/s00300-003-0482-3

Paxton, H., & Åkesson, B (2007) Redescription of *Ophryotrocha puerilis* and *O. labronica* (Annelida, Dorvilleidae). *Marine Biology Research*, *3*(1), 3–19. https://doi.org/10.1080/17451000601024373

Paxton, H., & Åkesson, B. (2010). The Ophryotrocha labronica group (Annelida: Dorvilleidae)—with the description of seven new species. *Zootaxa, 2713*(1), 1–24. https://doi.org/10.11646/zootaxa.2713.1.1

Pettibone, M. H. (1957). Endoparasitic polychaetous annelids of the family Arabellidae with descriptions of new species. *The Biological Bulletin, 113*(1), 170–187. https://doi.org/10.2307/1538811

Poddubnaya, L. G., Scholz, T., Kuchta, R., Levron, C., & Brunanská, M. (2007). Ultrastructure of the proglottid tegument (neodermis) of the cestode *Echinophallus wageneri* (Pseudophyllidea: Echinophallidae), a parasite of the bathypelagic fish *Centrolophus niger*. *Parasitology Research, 101*(2), 373–383. https://doi.org/10.1007/s00436-007-0475-1

Rambaut, A. (2018) FigTree v 1.4.4. http://github.com/rambaut/figtree/ Institute of Evolutionary Biology, University of Edinburgh.

Ritterson, A. L. (1966). Nature of the Cyst of Trichinella spiralis. *The Journal of Parasitology, 52*(1), 157–161. https://doi.org/10.2307/3276407

Rossi, M. M. (1984). A new genus and species of iphitimid parasitic in an aphroditid (Polychaeta), with an emendation of the family Iphitimidae. *Bulletin Southern California Academy of Sciences, 83*(3), 163–166.

Rouse, G. W. (2005). Annelid sperm and fertilization biology. *Hydrobiologia, 535*(1), 167–178. https://doi.org/10.1007/s10750-004-4390-5

Seixas, V. C., de Russo, C. A. M., & Paiva, P. C. (2017). Mitochondrial genome of the Christmas tree worm *Spirobranchus giganteus* (Annelida: Serpulidae) reveals a high substitution rate among annelids. *Gene, 605*, 43–53. https://doi.org/10.1016/j.gene.2016.12.024

Struck, T. H., Golombek, A., Hoesel, C., Dimitrov, D., & Elgetany, A. H. (2023). Mitochondrial genome evolution in Annelida - A systematic study on conservative and variable gene orders and the factors influencing its evolution. *Systematic Biology, 72*(4), 925–945. https://doi.org/10.1093/sysbio/syad023

Sun, Y., Daffe, G., Zhang, Y., Pons, J., Qiu, J.-W., & Kupriyanova, E. K. (2021). Another blow to the conserved gene order in Annelida: Evidence from mitochondrial genomes of the calcareous tubeworm genus *Hydroides*. *Molecular Phylogenetics and Evolution, 160*, 107124. https://doi.org/10.1016/j.ympev.2021.107124

Taboada, S., Wiklund, H., Glover, A. G., Dahlgren, T. G., Cristobo, J., & Avila, C. (2013). Two new Antarctic *Ophryotrocha* (Annelida: Dorvilleidae) described from shallow-water whale bones. *Polar Biology, 36*, 1031–1045. https://doi.org/10.1007/s00300-013-1326-4

Tempestini, A., Massamba-N'Siala, G., Vermandele, F., Beaudreau, N., Mortz, M., Dufresne, F., & Calosi, P. (2020). Extensive gene rearrangements in the mitogenomes of congeneric annelid species and insights on the evolutionary history of the genus *Ophryotrocha*. *BMC Genomics, 21*(1), 815. https://doi.org/10.1186/s12864-020-07176-8

Tilic, E., Bartolomaeus, T., & Rouse, G. W. (2016). Chaetal type diversity increases during evolution of Eunicida (Annelida). *Organisms Diversity & Evolution, 16*, 105–119. https://doi.org/10.1007/s13127-015-0257-z

Troyer, D., & Schwager, P. (1979). Ultrastructure and evolution of a sperm: Phylogenetic implications of altered motile machinery in *Ophryotrocha puerilis* spermatozoon. *European Journal of Cell Biology, 20*(2), 174–176.

Tyler, S., & Hooge, M. (2004). Comparative morphology of the body wall in flatworms (Platyhelminthes). *Canadian Journal of Zoology, 82*(2), 194–210. https://doi.org/10.1139/z03-222

Tyler, S., & Tyler, M. S. (1997). Origin of the epidermis in parasitic platyhelminths. *International Journal for Parasitology, 27*(6), 715–738. https://doi.org/10.1016/S0020-7519(97)00013-1

von Marenzeller, E. (1902). Südjapanische Anneliden. 3. Aphroditea, Eunicea. *Denkschriften Der Akademie Der Wissenschaften, Wien., 72*, 563–582.

Weigert, A., Golombek, A., Gerth, M., Schwarz, F., Struck, T. H., & Bleidorn, C. (2016). Evolution of mitochondrial gene order in Annelida. *Molecular Phylogenetics and Evolution, 94*(Pt A), 196–206. https://doi.org/10.1016/j.ympev.2015.08.008

Wiklund, H., Glover, A. G., & Dahlgren, T. G. (2009). Three new species of *Ophryotrocha* (Annelida: Dorvilleidae) from a whale-fall in the North-East Atlantic. *Zootaxa*, *2228*(1), 43–56. https://doi.org/10.11646/zootaxa.2228.1.3

Wiklund, H., Altamira, I. V., Glover, A. G., Smith, C. R., Baco, A. R., & Dahlgren, T. G. (2012). Systematics and biodiversity of Ophryotrocha (Annelida, Dorvilleidae) with descriptions of six new species from deep-sea whale-fall and wood-fall habitats in the north-east Pacific. *Systematics and Biodiversity, 10*(2), 243–259. https://doi.org/10.1080/14772000.2012.693970

Yen, N. K., & Rouse, G. W. (2020). Phylogeny, biogeography and systematics of Pacific vent, methane seep, and whale-fall *Parougia* (Dorvilleidae: Annelida), with eight new species. *Invertebrate Systematics, 34*(2), 200–233. https://doi.org/10.1071/IS19042

Zarowiecki, M., & Berriman, M. (2015). What helminth genomes have taught us about parasite evolution. *Parasitology*, *142*(S1), S85–S97. Cambridge University Press.

Zhang, D., Zhou, Y., Yen, N., Hiley, A. S., & Rouse, G. W. (2023). *Ophryotrocha* (Dorvilleidae, Polychaeta, Annelida) from deep-sea hydrothermal vents, with the description of five new species. *European Journal of Taxonomy, 864*, 167–194. https://doi.org/10.5852/ejt.2023.864.2101

Zhang, Y., Sun, J., Rouse, G. W., Wiklund, H., Pleijel, F., Watanabe, H. K., Chen, C., Qian, P. Y., & Qiu, J. W. (2018). Phylogeny, evolution and mitochondrial gene order rearrangement in scale worms (Aphroditiformia, Annelida). *Molecular Phylogenetics and Evolution, 125*, 220–231. https://doi.org/10.1016/j.ympev.2018.04.002